ISTU 2016

Program Booklet

The 16th International Symposium on Therapeutic Ultrasound

March 14–16, 2016
Dan Panorama Hotel, Tel Aviv, Israel

www.istu.org

Thermal Ablation

Co-Chairs: Vera Khokhlova, Marcia Costa
Hall A

84 ACCELERATION OF THERMAL ABLATION OF TISSUE VOLUMES IN HIGH INTENSITY FOCUSED ULTRASOUND THERAPY USING SHOCK WAVE EXPOSURES

Vera A. Khokhova[1, 2], Peter V. Yuldashev[1], Ilya Sinilshchikov[1], Yulia Andriyakhina[1], Tatiana D. Khokhlova[4], Wayne Kreider[2], Adam Maxwell[5], Oleg Sapozhnikov[1, 2], Ari Partanen[3]

[1]Physics Faculty, M.V. Lomonosov Moscow State University, Moscow, Russian Federation, [2]Center for Industrial and Medical Ultrasound, University of Washington, Seattle, Washington, United States, [3]Clinical Science MR Therapy, Philips, Andover, Massachusetts, United States, [4]Dept. of Gastroenterology, School of Medicine, University of Washington, Seattle, Washington, United States, [5]Dept. of Urology, School of Medicine, University of Washington, Seattle, Washington, United States

OBJECTIVES

In high intensity focused ultrasound (HIFU) applications, nonlinear acoustic effects can result in the formation of high-amplitude shock fronts in focal waveforms, with amplitudes that can exceed 100 MPa. The presence of such shocks leads to increased tissue heating and initiation of boiling in milliseconds. Even though this shock-wave heating is very strong, shock fronts are highly focused and produce extreme heating effects in a very small focal volume. For single lesions, nonlinear heating thus can be utilized for rapid tissue ablation only within very small volumes before boiling starts to change the process. However, if the focus is steered, this enhanced heating combined with thermal diffusion can be used to accelerate thermal treatments over large volumes. The goal of this work was to evaluate the efficacy of using shock-wave heating to accelerate the thermal ablation of tissue volumes while keeping the same exposure conditions for intervening tissues.

METHODS

Simulation studies were performed for a multi-element 1.2 MHz HIFU phased array of a clinical system (Figure 1a, Sonalleve V1, Philips, Vantaa, Finland). Several acoustic power levels were considered within the possible range of array
outputs from 104 W to 1300 W, corresponding to intensities at the array elements from 1.2 W/cm^2 to 15 W/cm^2. A pulsing scheme was combined with discrete electronic steering of the array focus over a series of targets arranged in circles with radii of 2 and 4 mm (Figure 1b) to generate volumetric lesions in *ex vivo* bovine tissue. Point numbers in the sonication sequence are indicated in the Figure 1b. The circles were positioned in a plane at 25 mm depth in a bovine liver tissue sample of 50 mm thickness (Figure 1c), and the period between consecutive pulses was 40 ms.
Acoustic field in tissue was modelled using the Westervelt equation and a previously developed finite-difference algorithm. Temperature modelling in tissue was conducted using the bioheat equation with heat sources calculated from the acoustic modelling. Temperature simulations were optimized in the following way. First, the effect of a sonication at a single focus was computed in the time domain on a fine grid, which covered only the focal volume until the diffused temperature distribution was broad enough to be transferred to a sparser grid that covered the entire tissue sample. Second, volumetric modelling of the bioheat equation was conducted on the sparser grid in a spatial-frequency domain where an analytic solution is available. Based on the linearity of the bioheat equation, the temperature distribution calculated at the first step was added to the current temperature distribution in

tissue at each consecutive steering position of the focus with the time delay equal to the heating and diffusion time of the sonication in a single focus.
Temperature simulations were conducted for a constant time-average intensity at the array elements, considering either a peak intensity of 1.2 W/cm^2 over a HIFU pulse duration of 20 ms, 8 W/cm^2 over a duration of 3 ms, or 15 W/cm^2 over a duration of 1.6 ms. For comparison, the initial intensity of 1.2 W/cm^2 corresponds to a total acoustic output power of 104 W. Sonication of targets was performed starting from the centre of the circles spiraling outward and continued until the minimum temperature rise inside the circle of 4 mm radius in the focal plane reached 45°C. Assuming *ex vivo* exposures with initial temperature of 20°C, this temperature rise is representative for tissue denaturation within the irradiated volume. Here we term the focal plane as the plane of the maximum heat deposition for each intensity output. To equalize the temperature over each circle, the distribution of sonication points was rotated with each consecutive cycle to irradiate locations in between the sonication points of the previous cycle (Figure 1b).

RESULTS

Shown in Figure 2 are waveforms simulated at the position of maximum heat deposition in tissue for different peak intensities at the array elements from 1.2 to 15 W/cm^2. These output levels corresponded to quasilinear sonication (1.2 W/cm^2, red curve), sonication with a fully developed shock of 95 MPa at the focus (8 W/cm^2, pink curve), and sonication with a higher focal shock amplitude of 118 MPa (15 W/cm^2, blue curve).
Shown in Figure 3 are spatial distributions of heat deposition rates in tissue in the axial plane of the array simulated for different peak intensities at the array elements. Heat depositions are normalized relative to the heat deposition calculated for the same intensities assuming linear wave propagation. It is seen that at 8 W/cm^2 with a shock front of about 100 MPa, the tissue heating at the focus is about 35 times higher than predicted linearly and is highly localized in space. With further increase of the intensity to 15 W/cm^2, the shock front at the focus is about 120 MPa resulting in 40 times more effective heating. In addition, the region of the presence of high-amplitude shock and therefore enhanced heating is enlarged.
Corresponding temperature distributions in the focal plane are shown in Figure 4 at times when the temperature rise inside the circle of 4 mm radius reaches 45°C. For the lowest peak intensity (1.2 W/cm^2) this temperature level was reached in 84 seconds. For higher outputs it required 34 and 13 seconds, correspondingly, showing significant acceleration of the treatment. At higher peak intensities, the volumetric temperature rise occurred more quickly while the boundary between treated and untreated tissue became more clearly defined.

CONCLUSIONS

HIFU irradiations of tissue volume in three different nonlinear regimes were considered. It was shown that with the same time-average power, the use of pulsing schemes with higher peak power leads to faster heating of the desired volume and less heat diffusion to the surrounding tissues. Such regimes therefore show clinical advantages to accelerate thermal HIFU therapy while keeping the same safe exposure conditions for surrounding tissues and sharper margins of treatment. The study was supported by the RSF 14-12-00974, NIH NIBIB EB007643, and student Global Internship Program from the Focused Ultrasound Foundation.

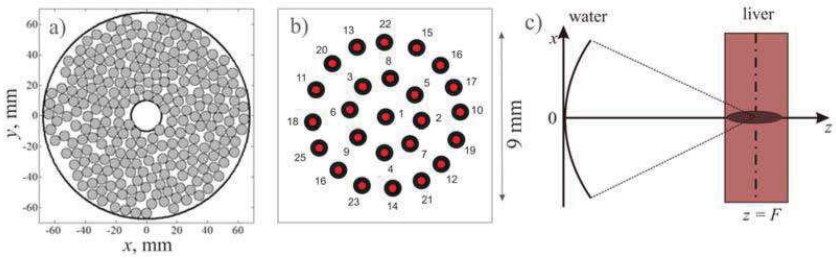

Figure 1: (a) Distribution of radiating elements on the surface of the therapeutic array; (b) Discrete trajectory of the beam's focus in the focal plane. (c) Geometry of the numerical experiment: ultrasound beam is focused within tissue layer (liver) of 5 cm thickness centred at the geometric focus of the spherical shell. Acoustical modelling was performed both in water and in liver sample, while temperature modelling was performed only in liver.

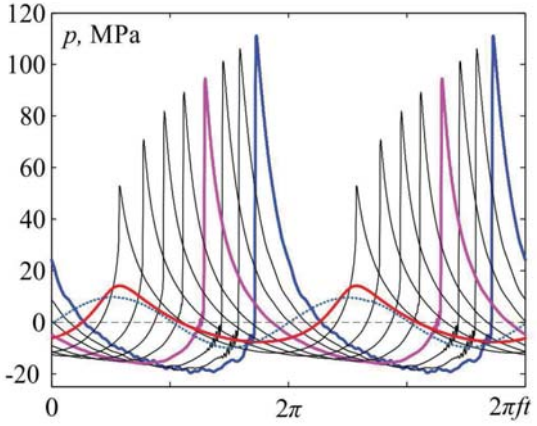

Figure 2: Acoustic pressure waveforms simulated at the maximum of heat deposition in tissue for different intensities at the array elements: 1.2 W/cm^2 (red curve), 4, 5, 6, 7, 8 W/cm^2 (pink curve), 10, 12, and 15 W/cm^2 (blue curve). Dashed curve is the focal waveform for 1.2 W/cm^2 simulated linearly. While quasilinear regime of focusing with slightly distorted focal waveform is realized for initial intensity of 1.2 W/cm^2, high amplitude shocks are formed at intensities of 8 W/cm^2 (95 MPa) and 15 W/cm^2 (118 MPa).

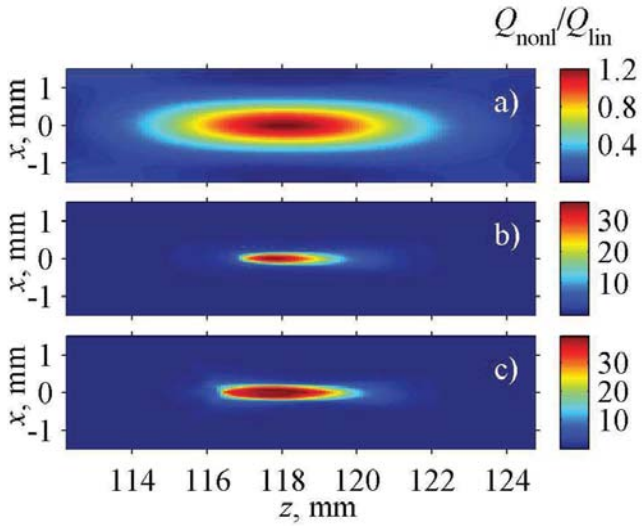

Figure 3: Spatial 2D distributions of heat deposition rates in tissue in the axial plane of the array for different intensities at the array elements: (a) 1.2 W/cm^2, (b) 8 W/cm^2, and (c) 15 W/cm^2. Heat deposition rates are normalized to the heating rates calculated at the same intensities assuming linear wave propagation conditions. The distributions therefore illustrate nonlinear enhancement and better spatial localization of heating using shock-wave exposures.

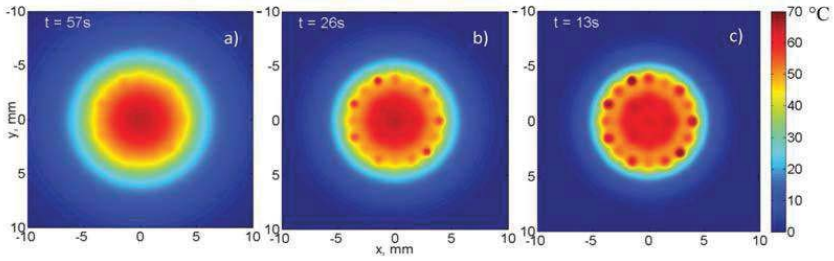

Figure 4: Spatial 2D distributions of temperature rise in tissue in the plane of maximum heat deposition for different peak intensities at the array elements balanced by the pulse length within 40 ms time window between the pulses: (a) 1.2 W/cm^2 and 20 ms, (b) 8 W/cm^2 and 3 ms, and (c) 15 W/cm^2 and 1.6 ms. As indicated in each frame, temperature maps are shown at the time point when temperature rise everywhere inside the circle of 4 mm radius reaches 45°C. This temperature rise would ensure tissue denaturation for *ex vivo* exposures with initial tissue temperature of 20°C.

85 ULTRASONIC HEMOSTATSIS OF DEEP ARTERIAL BLEEDING

Andrey Rybyanets[1], *Natalia Shvetsova*[1], *Alex Berkovich*[2], *Igor Shvetsov* [1], *Oleg Sapozhnikov*[3], *Vera Khokhlova*[3]

[1]Southern Federal University, Rostov on Don, Russian Federation, [2]Saint Petersburg Polytechnical University, Saint Petersburg, Russian Federation, [3]Moscow State University, Moscow, Russian Federation

OBJECTIVES

Ultrasonic hemostasis may provide an effective method in surgery and prehospital settings for treating trauma and elective surgery patients. Application of HIFU therapy to hemostasis was primarily initiated in an attempt to control battlefield injuries on the spot. High-intensity focused ultrasound (HIFU) has been shown capable of coagulation of internal bleeding. The main drawback of the thermal hemostasis strategy is low ultrasound absorption ability of blood and, as a result, low heating and coagulation rate at real blood flow.
The purpose of this study was to evaluate the feasibility of HIFU thermal and combinational (cavitation, boiling, non-linear behaviors, and coagulation agents) effects for ultrasonic hemostasis of deep arterial bleeding.

METHODS

In this paper, HIFU therapy and imaging transducer designs, nonlinear acoustic fields modelling and calculations, as well as in vivo hemostasis experiments on lamb's femoral artery confirming enhanced ultrasonic hemostasis at deep arterial bleeding are described. For ex vivo and in vivo hemostasis experiments an ultrasonic applicator was designed and tested. The ultrasonic applicator design had HIFU therapy transducer and imaging probes and was configured to be compatible with 3D mechanical scanning system. HIFU transducers are comprised 1-2 MHz spherical elements made from porous piezoceramics with 80 mm aperture having radius of curvature 40-60 mm. Centre opening with 40 mm diameter was reserved for ultrasonic imaging and Doppler probes such as linear, convex or 3D arrays.
Acoustic measurements of ultrasonic transducers have been performed in 3D Scanning System (UMS3) using the fiber optic hydrophone (FOPH 2000) and using AFB from Precision Acoustics Ltd. Waveforms from the hydrophones and the driving voltage were recorded using a digital oscilloscope Lecroy. The transducer was driven by a function generator Agilent 33521B, a linear RF amplifier E&I model 2400L RF, and operates in a CW or burst modes. The acoustic intensity in the focal
plane measured in water tank at 1000-5000 W/cm^2 (ISAL) was kept for the objects treatment. The experiments were made on acoustic vascular phantoms, as well as on lamb's femoral artery in vivo at different protocols. During ultrasound exposure of lamb's femoral artery, arterial blood flow was temporarily stopped using intravascular balloon. In some protocols intravenous coagulation agents (liposomes) activated by HIFU at the point of bleeding were used. Targeting accuracy was assessed by necropsy and histologic exams and efficacy (vessel thrombosis) by angiography and histology.